Interacting spin-$\frac{1}{2}$ tetrahedral system $Cu_2Te_2O_5X_2$ (X=Cl,Br): A mean-field and random phase approximation analysis

Jens Jensen
Niels Bohr Institute, Universitetsparken 5, 2100 Copenhagen, Denmark
(Received 20 October 2008; published 7 January 2009)

Magnetic ordering and excitations of $Cu_2Te_2O_5Cl_2$ are analyzed in terms of a tetramerized spin model for the tetrahedral Cu clusters of spin 1/2. The mean-field model is able to account for the main properties of the incommensurable magnetic structure observed by Zaharko *et al.* [Phys. Rev. B **73**, 064422 (2006)]. The calculated excitation spectra show many similarities with the experimental neutron-scattering results. Close to a magnetic Bragg point at 2 K, the theory predicts the presence of a quasielastic phason mode and an inelastic amplitude mode at about 0.6 meV. This is in qualitative agreement with experimental observations of Prša *et al.*, but the amplitude mode is observed at the much higher energy of about 2.5 meV. This discrepancy is puzzling since the tetrahedral Cu-spin system, in any other respect, behaves as a system of large local spins coupled with each other in a three-dimensional fashion. Preliminary model calculations for the $Cu_2Te_2O_5Br_2$ system lead to the same conclusion.

DOI: 10.1103/PhysRevB.79.014406 PACS number(s): 75.10.−b, 75.30.Ds

I. INTRODUCTION

The crystal structure of $Cu_2Te_2O_5Cl_2$ was determined by Johnsson *et al.*[1] It belongs to the tetragonal space group $P\bar{4}$ (No. 81) with a=7.621 Å and c=6.320 Å, and the Cu ions are placed at the positions Cu-1 (x,y,z), Cu-2 $(1-x,1-y,z)$, Cu-3 $(y,1-x,-z)$, and Cu-4 $(1-y,x,-z)$, where x=0.731, y=0.453, and z=0.158 (in units of the lattice parameters). The crystal structure projected on the *ab* and *ac* planes is shown in Fig. 1, and it contains clusters of Cu ions aligned in tubes along the *c* direction. The four Cu ions lying closest to each other form a distorted tetrahedron. The spins of the Cu^{++} ions are $S=\frac{1}{2}$, and the system is ideal for studying frustration effects due to intratetrahedral spin interactions competing with the exchange interactions between spins on neighboring tetrahedra. In contrast to the pyrochlore lattice antiferromagnets, which are geometrically frustrated because the tetrahedra are sharing corners,[2] the tetrahedra formed here are separate units. The high-temperature susceptibility of $Cu_2Te_2O_5Cl_2$ approaches that of uncoupled spins, and at low temperatures the susceptibility is reduced and goes through a maximum at about 23 K.[1] The maximum indicates that the 16 spin-1/2 states of the Cu ions in each tetrahedron are tetramerized so to create a singlet ground state separated from the excited states by a gap of about 40 K.

The susceptibility and heat-capacity measurements clearly indicate a transition to an ordered phase at a temperature of about 18.2 K.[3,4] The phase was anticipated to be a simple ferromagnetic or antiferromagnetic ordering of the tetrahedral cluster spins, but neutron-diffraction measurements by Zaharko *et al.*[5] surprisingly revealed a much more complex situation—that the Cu spins in the Cl system were ordered at the incommensurable wave vector $\mathbf{Q}=(-0.150,0.422,0.5)$. Recent diffraction measurements utilizing polarized neutrons have led to a detail determination of the spin structure.[6] The ith tetrahedron is specified by the lattice vector $\mathbf{R}_i$ of the unit cell in which Cu-1 and Cu-2 are lying. The ordered spin of the Cu-α ion in this tetrahedron is then described by the following equation:

$$\langle \mathbf{S}_{\alpha i} \rangle = S_0[\hat{\mathbf{x}} \cos(\mathbf{Q}\cdot\mathbf{R}_i + \psi_\alpha) + \hat{\mathbf{z}} \sin(\mathbf{Q}\cdot\mathbf{R}_i + \psi_\alpha)], \quad (1)$$

where $\hat{\mathbf{z}}$ is a unit vector along the *c* axis and $\hat{\mathbf{x}}$ is a unit vector in the *ab* plane making an angle ϕ with the *a* axis. Hence, all the four ordered spins of a certain tetrahedron are lying in the same *xz* plane, which spins rotate from one tetrahedron to the next as described by the wave vector $\mathbf{Q}$. The *xz* plane of the moments is not perpendicular to $\mathbf{Q}$, as in the case of a genuine helix, however, the polarization is nearly perpendicular to the projection of $\mathbf{Q}$ on the *ab* plane ($\mathbf{Q}$ makes an angle of 110° with the *a* axis). At 2 K, the amplitude S_0 is found to be 0.44 and ϕ is about 14°, and assuming $\psi_1=0$, the three other phase angles are determined to be $\psi_2=13°$, $\psi_3=-136°$, and $\psi_4=154°$. Notice that the four Cu ions specified by α=1, 2, 3, 4 in Eq. (1) are all belonging to the same tetrahedron, but only the Cu-1 and Cu-2 ions are lying in the unit cell specified by $\mathbf{R}_i$. In Table III of Ref. 6, the Cu-3 and Cu-4 ions are those belonging to the neighboring Cu tetrahedron along the *c* axis but lying in the same unit cell as the two other ions. This definition adds an extra 180° to the phases ψ_3 and ψ_4.

The lattice parameters *a* and *c* of the isostructural $Cu_2Te_2O_5Br_2$ compound are increased by, respectively, 2.8% and 0.9% in comparison with the Cl compound. The volume of the tetrahedral Cu unit shows the opposite modification by being reduced by about 3%. These changes imply that the gap between the singlet ground state and the excited states of the tetrahedral is increased, whereas the intertetrahedral interactions are reduced. The effective intertetrahedral coupling, responsible for inducing a magnetic ordering of the singlet ground-state system, exceeds the threshold value by about a factor of 2 in the case of the Cl system. The Br compound is closer to quantum criticality, as the effective interaction is here only about 15% larger than the critical value. The Br compound is observed to order[6] at 11.4 K at the wave vector $(-0.172,0.356,0.5)$ in a structure described by Eq. (1) with an amplitude at 2 K of S_0=0.20. The angle between the *x* and *a* axes is now $\phi=9°$ and the phase angles are $\psi_2=22°$, $\psi_3=-105°$, and $\psi_4=134°$.

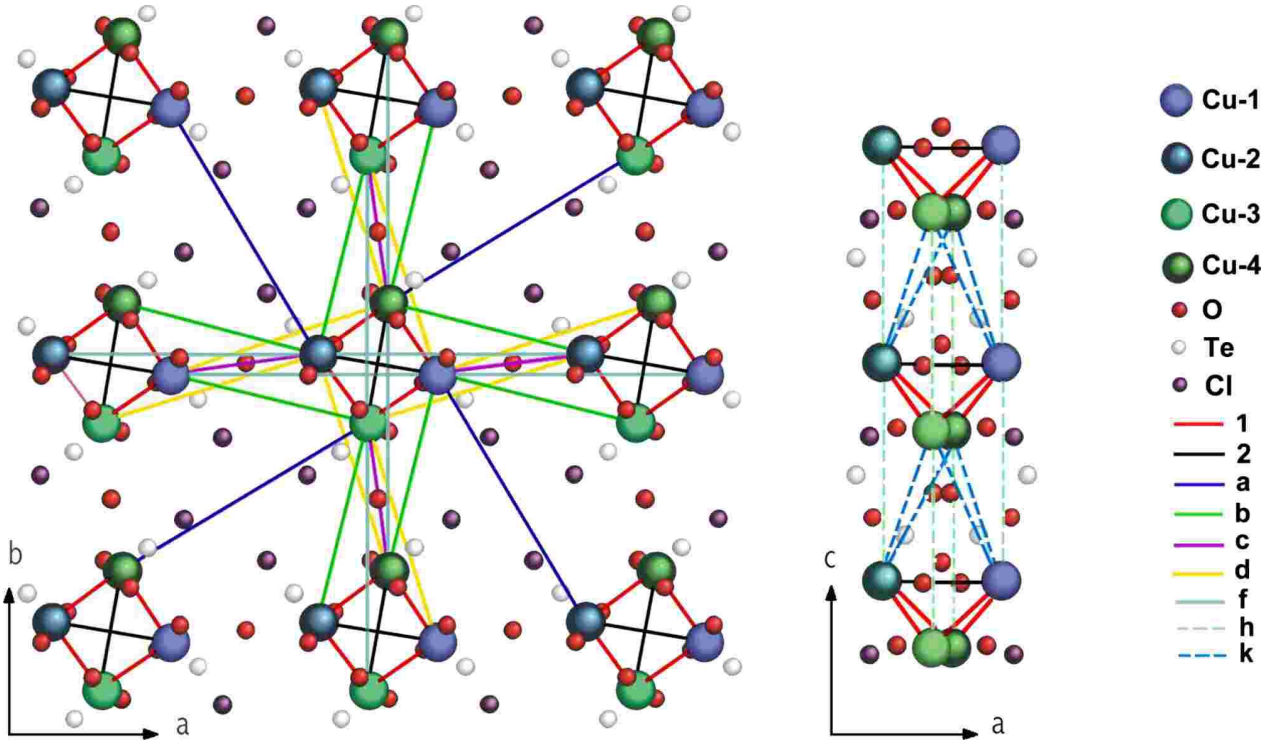

FIG. 1. (Color online) The $Cu_2Te_2O_5Cl_2$ crystal projected on the *ab* and *ac* planes. The intratetrahedral interactions J_1 and J_2 are indicated by the red and black lines, respectively. The intertetrahedral interactions between the central tetrahedron and its surroundings, J_a-J_k, are indicated by colored lines according to the specifications to the right.

Here, I shall mostly concentrate on the Cl compound. The mean-field (MF) model for describing the magnetic ordering of this compound is developed in Sec. II. The magnetic excitations predicted by this model and calculated within the random phase approximation (RPA) are analyzed in Sec. III. In Sec. IV, I present a condensed version of the similar analysis performed on the Br compound. The results achieved by the MF/RPA models of the two tetramerized compounds are summarized in Sec. V.

II. MEAN-FIELD MODEL OF $Cu_2Te_2O_5Cl_2$

The bulk properties and the Raman-scattering results of $Cu_2Te_2O_5Cl_2$ and of the Br compound were analyzed successfully by Gros *et al.*[7] and Jensen *et al.*[8] in terms of a tetramerized model for the four Cu spins of one tetrahedron. The model in Ref. 8 is utilized here as the starting point for the MF analysis. In accordance with the S_4 symmetry of the crystal, the Hamiltonian of the four Cu spins of one tetrahedron is considered to be

$$\begin{aligned}\mathcal{H}_t &= J_1(\mathbf{S}_1+\mathbf{S}_2)\cdot(\mathbf{S}_3+\mathbf{S}_4)+J_2(\mathbf{S}_1\cdot\mathbf{S}_2+\mathbf{S}_3\cdot\mathbf{S}_4)\\ &+ D_1[\cos\theta_D(S_1^aS_3^c-S_1^cS_3^a+S_2^cS_4^a-S_2^aS_4^c)\\ &+ \sin\theta_D(S_1^cS_4^a-S_1^aS_4^c+S_2^aS_3^c-S_2^cS_3^a)\\ &+ \cos\theta_D(S_1^bS_4^c-S_1^cS_4^b+S_2^cS_3^b-S_2^bS_3^c)\\ &+ \sin\theta_D(S_1^bS_3^c-S_1^cS_3^b+S_2^cS_4^b-S_2^bS_4^c)],\end{aligned} \tag{2}$$

where $\mathbf{S}_\alpha$ is the SU(2) spin operator at site α with the component S_α^ξ along the ξ axis. The coupling parameters are found to be

$$J_1=40.9\ \text{K},\quad J_2=J_1,\quad D_1=0.03J_1,\quad \theta_D=55.6^\circ. \tag{3}$$

In the previous model the Dzyaloshinsky-Moriya (DM) anisotropy, $\mathbf{D}_{\alpha\beta}\cdot\mathbf{S}_\alpha\times\mathbf{S}_\beta$, was assumed to be dominated by the term, where $\mathbf{D}_{\alpha\beta}$ is parallel to the *c* axis.[8] Since then, the plane of the moments has been determined to be perpendicular to the *ab* plane.[6] In this situation the *c*-axis term may be neglected in comparison with the present DM term, where $\mathbf{D}_{\alpha\beta}$ is perpendicular to the *c* axis. The local symmetry indicates that the intratetrahedral DM vector ($\alpha=1$, 2 and $\beta=3$, 4) should be approximately perpendicular to the plane determined by $\mathbf{r}_\alpha-\mathbf{r}_\beta$ and the *c* axis.[9,10] This is not an exact symmetry, and $\mathbf{D}_{\alpha\beta}$ is allowed to point in a somewhat different direction in the *ab* plane by introducing a θ_D, which is different from the angle of 33.5° between the *ab* component of $\mathbf{r}_1-\mathbf{r}_3$ and the *a* axis.

The total Hamiltonian includes $\mathcal{H}_t$ of each tetrahedron, the exchange interactions between the single spins of each tetrahedron and those of the neighboring ones, the Zeeman term, and the classical dipole-dipole interaction,

$$\begin{aligned}\mathcal{H}=\sum_i\mathcal{H}_t(i)+\frac{1}{2}\sum_{\alpha i,\beta j}J_{ij}^{\alpha\beta}\mathbf{S}_{\alpha i}\cdot\mathbf{S}_{\beta j}-\sum_{\alpha i}2\mu_B\mathbf{H}\cdot\mathbf{S}_{\alpha i}\\ -\frac{1}{2}(2\mu_B)^2\sum_{\alpha i,\beta j}\sum_{\xi\eta}D^{\xi\eta}(\alpha i,\beta j)S_{\alpha i}^\xi S_{\beta j}^\eta.\end{aligned} \tag{4}$$

$S_{\alpha i}^\xi$ denotes the ξth Cartesian component of $\mathbf{S}_{\alpha i}$ at the position $\mathbf{r}_{\alpha i}$ and

$$D^{\xi\eta}(\alpha i,\beta j)=\frac{3(r^{\xi}_{\alpha i}-r^{\xi}_{\beta j})(r^{\eta}_{\alpha i}-r^{\eta}_{\beta j})-|\mathbf{r}_{\alpha i}-\mathbf{r}_{\beta j}|^2\delta_{\xi\eta}}{|\mathbf{r}_{\alpha i}-\mathbf{r}_{\beta j}|^5}. \quad (5)$$

The dipole-dipole interaction is weak compared to the exchange, but it is anisotropic. The interesting feature of this anisotropy term is that it predicts an orientation of the plane of the moments close to that observed experimentally. However, in comparison to the DM term D_1 of the order of a few percent of J_1, the classical anisotropy is of no importance and may be left out of the model. The exchange-interaction parameters $J^{\alpha\beta}_{ij}$ considered in the model are defined in Fig. 1 and comprise seven different couplings $J_a,\ldots,J_k$. The total number of model parameters is 11. The previous analysis determines 3–4 of these from susceptibility, magnetization, and Raman-scattering measurements.[8] The properties of the ordered phase (T_N, $\mathbf{Q}$, and the amplitude of the ordered moments) imply 3–4 more constraints. This leaves about 4 extra degrees of freedom which have been utilized for various purposes to be discussed below. In the model calculations, the intratetrahedral interactions have been accounted for in an exact way, whereas the intertetrahedral interactions have been treated in the mean-field approximation, $S^{\xi}_{\alpha i}S^{\eta}_{\beta j}\simeq S^{\xi}_{\alpha i}\langle S^{\eta}_{\beta j}\rangle+\langle S^{\xi}_{\alpha i}\rangle S^{\eta}_{\beta j}-\langle S^{\xi}_{\alpha i}\rangle\langle S^{\eta}_{\beta j}\rangle$, when $i\neq j$. The magnetic ordering is presumably incommensurable, but in order to carry out the calculations I need to assume a commensurable structure. I have considered various possibilities, and the smallest, but still acceptably realistic choice, is a lattice of $7\times7\times2$ tetrahedra, in which case the ground-state wave vector $\mathbf{Q}=(-\frac{1}{7},\frac{3}{7},\frac{1}{2})\simeq(-0.143,0.429,0.5)$ is reasonably close to the experimental value. Introducing the MF approximation in Eq. (4), the Hamiltonian of the ith of the $7\times7\times2$ different tetrahedra in one commensurable period is diagonalized and the thermal expectation values $\langle S^{\xi}_{\alpha i}\rangle$ are calculated. This calculation is repeated until self-consistency is attained. When the equilibrium configuration has been establish, the "noninteracting" susceptibility tensor[11] of the jth tetrahedron is determined [in units of $(g\mu_B)^2$] by

$$\chi^0_{AB}(j,\omega)=\lim_{\epsilon\to0^+}\left[\sum_{ab}^{E_a\neq E_b}\frac{\langle a|A|b\rangle\langle b|B|a\rangle}{E_b-E_a-\hbar(\omega+i\epsilon)}(n_a-n_b)+\frac{1}{k_BT}\left(\frac{i\epsilon}{\omega+i\epsilon}\right)^2\times\left\{\sum_{ab}^{E_a=E_b}\langle a|A|b\rangle\langle b|B|a\rangle n_a-\langle A\rangle\langle B\rangle\right\}\right]. \quad (6)$$

A or B is one of the 4×3 spin operators $S^{\xi}_{\alpha j}$, and E_a, $|a\rangle$, and n_a are the ath eigenvalue, eigenstate, and population factor, respectively, of the MF Hamiltonian for the jth tetrahedron.

In order to derive a set of interaction parameters, which predict the right ordering wave vector at T_N, I have utilized that the characteristic determinant vanishes at the second-order phase transition or, approximately, that

$$\left|\delta_{\alpha\beta}-\sum_{\gamma}\chi^0_{\alpha\gamma}(j,0)|^{\xi\xi}J^{\gamma\beta}(\mathbf{Q})\right|\to0^+ \quad (7)$$

for $T\to T_N^+$, when neglecting the minor effects of the anisotropy terms. In the paramagnetic phase, $\bar{\bar{\chi}}^0_{\alpha\beta}(j,0)$ is independent of the tetrahedron considered and approximately diagonal with respect to the Cartesian components (ξ is equal to a, b, or c) and

$$J^{\alpha\beta}(\mathbf{q})=\sum_k J^{\alpha\beta}_{jk}e^{-i\mathbf{q}\cdot(\mathbf{R}_j-\mathbf{R}_k)}. \quad (8)$$

TABLE I. The structure parameters of $Cu_2Te_2O_5X_2$ at 2 K. The upper part applies to X=Cl and the lower one to X=Br. All angles are in degrees. In the calculations $\phi_1=\phi_2$ is found to differ from $\phi_3=\phi_4$ but only by about 0.15°. The remaining angles not included in the table are $\psi_1=0$, $\theta_2=-\theta_1$, and $\theta_4=-\theta_3$. The experimental values are determined by the neutron-diffraction experiments of Zaharko *et al.* (Ref. 6).

	S_0	ϕ_α	θ_1	θ_3	ψ_2	ψ_3	ψ_4
Calc.	0.436	14	−1.2	−0.1	3.9	−153.6	157.5
Expt.	0.44	14			13	−136	154
Calc.	0.205	9	−1.9	−1.0	12.1	−159.2	171.3
Expt.	0.20	9			22	−105	134

The model to be discussed below is determined by the parameters in Eq. (3) and by the following values for the coupling parameters defined in Fig. 1:

$$J_a=0.8,\quad J_b=-0.1,\quad J_c=-0.1,\quad J_d=-0.3,$$

$$J_f=-0.03,\quad J_h=0.1,\quad J_k=-0.42, \quad (9)$$

in units of J_1. Notice that the coupling parameters with a negative sign are the ferromagnetic ones. The ordered structure determined by this model is similar to the one determined from polarized-neutron diffraction [Eq. (1)], though there are some subtle differences, which are, however, difficult to detect experimentally. The calculated polarization is not precisely circular, but the lengths of the two semiaxes differ by less than 0.5%, which slight eccentricity is neglected. More significant modifications are that the plane of the moments is different for the four different magnetic sublattices and that these planes are tilted small angles away from the c axis. Hence, instead of Eq. (1), the calculated structures are described by the following expression:

$$\langle\mathbf{S}_{\alpha i}\rangle=S_0[\hat{\mathbf{x}}_\alpha\cos(\mathbf{Q}\cdot\mathbf{R}_i+\psi_\alpha)+\hat{\mathbf{z}}_\alpha\sin(\mathbf{Q}\cdot\mathbf{R}_i+\psi_\alpha)], \quad (10)$$

where $\hat{\mathbf{x}}_\alpha$ lies in the ab plane making the angle ϕ_α with the a axis, and $\hat{\mathbf{z}}_\alpha$ is tilted an angle θ_α away from the c axis within the plane normal to $\hat{\mathbf{x}}_\alpha$. The spin components in the abc coordinate system are determined from the xyz components (and $\langle S^y\rangle\equiv0$) according to

$$\langle S^a\rangle=\langle S^x\rangle\cos\phi+\langle S^z\rangle\sin\theta\sin\phi,$$

$$\langle S^b\rangle=\langle S^x\rangle\sin\phi-\langle S^z\rangle\sin\theta\cos\phi,$$

$$\langle S^c\rangle=\langle S^z\rangle\cos\theta. \quad (11)$$

The calculated results for the structure parameters defined by Eq. (10) are shown in Table I when using the model defined

above, i.e., Eqs. (3) and (9) in the case of $\mathbf{Q}=(-\frac{1}{7},\frac{3}{7},\frac{1}{2})$ and $T=2$ K. By calculating the free energies of structures with various commensurable periods it is found that the true ordering wave vector of the model depends on temperature. It is $(-0.157,0.414,0.5)$ just below T_N and close to $(-\frac{6}{41},\frac{18}{41},\frac{1}{2})=(-0.146,0.439,0.5)$ at 2 K. Experimentally,[5] the temperature dependence of $\mathbf{Q}$ is much weaker, and I have chosen a set of parameters so that the calculated $\mathbf{Q}$ is relatively close to the experimental one both at 2 K and at T_N. The calculated structure parameters depend on the choice of $\mathbf{Q}$, but the changes are small and unimportant as long as the assumed commensurable (metastable) structure has a $\mathbf{Q}$ in the neighborhood of the true ordering wave vector. The calculated structures may exhibit the presence of higher harmonics, but in the present model they are of no significance. The diffraction experiments do not show any indications of higher harmonics,[12] and when developing the model I have aimed at minimizing their importance.

At zero field the two domains with the ordering wave vectors $\mathbf{Q}=(Q_a,Q_b,0.5)$ and $\mathbf{Q}_\perp=(Q_b,-Q_a,0.5)$ are degenerated. Experimentally, the application of a field of the order of 5 kOe parallel to $\mathbf{Q}$ removes the $\mathbf{Q}_\perp$ domain.[12] The model calculations indicate that the system has a strong tendency toward developing a double-$\mathbf{Q}$ structure, where the $\mathbf{Q}$ domain has an additional component polarized nearly along the b axis and modulated with the wave vector $\mathbf{Q}_\perp$. If modifying the model slightly, $J_f=0$ and $D_1=0.003J_1$ while the remaining parameters are unchanged; the amplitude of the $\mathbf{Q}_\perp$ component is found to be 0.3 times the $\mathbf{Q}$ component at 2 K. The double-$\mathbf{Q}$ component is nearly unaffected by a field of 5 kOe and is only removed at fields which are ten times larger. At zero field, the $\mathbf{Q}_\perp$ order component is stable nearly up to T_N (within the numerical accuracy). In the final model [Eq. (9)], the $\mathbf{Q}_\perp$ component is eliminated at all temperatures, and the number and amplitudes of the higher harmonics are simultaneously reduced, which features are in accordance with the experimental observations. However, as we shall see, the calculated excitation spectrum indicates that the system is nearly soft with respect to the creation of the double-$\mathbf{Q}$ component.

The possible higher harmonics in the case of a commensurable structure with the dimensions $\tau_1\times\tau_2\times\tau_3$ are at the wave vectors

$$\mathbf{Q}_\mathbf{p}=\left(\frac{p_1}{\tau_1},\frac{p_2}{\tau_2},\frac{p_3}{\tau_3}\right),\quad p_i=0,1,\ldots,\tau_i-1 \tag{12}$$

modulo a reciprocal-lattice vector. Incidentally, in the case of the tetragonal $7\times7\times2$ lattice, the $\mathbf{Q}_\perp$ component may equally well be classified as a higher harmonic. That it is a genuine double-$\mathbf{Q}$ component may be checked by choosing, for instance, a $40\times40\times2$ lattice with $\mathbf{Q}=(-\frac{6}{40},\frac{17}{40},\frac{1}{2})=(\frac{17}{20},\frac{17}{40},\frac{1}{2})$, where $\mathbf{Q}_\perp=(\frac{17}{40},\frac{3}{20},\frac{1}{2})$ is not among the wave vectors of the higher harmonics.

The calculated structure has many features in common with the magnetic structure derived from the polarized-neutron-diffraction experiment. The orientation angle of the DM vectors, θ_D, has been adjusted so that the orientation of the plane of the moments is in agreement with experiment when neglecting the small tilting angles θ_α. The spins of Cu-1 and Cu-2 are nearly parallel to each other and nearly antiparallel to the spins of Cu-3 and Cu-4. The calculated angles $\alpha_{12}=4°$, between the spins of Cu-1 and Cu-2, and $\alpha_{34}=49°$, between the spins of Cu-3 and Cu-4, differ somewhat from the experimental values of $\alpha_{12}=13°$ and $\alpha_{34}=70°$. I have tried to improve on this, but it turned out to be difficult to get any appreciable changes in the values of these angles. Actually, the calculated structure is rather robust against even major changes in the interaction parameters in Eq. (9), as long as they predict the right T_N and $\mathbf{Q}$. The tilting angles θ_α are proportional to the DM anisotropy. If the sign of D_1 is changed, these angles change sign. The presence of the DM anisotropy implies that only one chiral domain is stable. The chirality chosen in Eq. (10) corresponds to a positive value of D_1. If this coupling constant is negative, the sign in front of $\hat{\mathbf{z}}_\alpha$ Eq. (10) should be changed from plus to minus. The prediction that only one of the two choices is stable, as determined by the sign of D_1, is concordant with the experimental observation of Zaharko *et al.*[6] that the two chiral domains are "unequally populated."

The previous analysis[8] indicated that $J_2\approx J_1$, which is in agreement with the present indications. J_2 cannot be much larger than J_1 since that would lead to an ordered structure, where $\langle\mathbf{S}_1\rangle$ and $\langle\mathbf{S}_2\rangle$ are (nearly) antiparallel instead of parallel to each other. If adjusting the other exchange parameters, the ordered structure may equally well be reproduced if choosing a smaller J_2, except for one property. The zero-point reduction in the ordered moment is found to increase in proportion to the reduction in J_2/J_1 when adjusting the other coupling parameters so to keep T_N and $\mathbf{Q}$ fixed. Assuming $J_2/J_1=0.9$ instead of 1, the amplitude is calculated to be reduced from $S_0=0.436$ to about 0.42. A comparison of this result to the experimental value of $2S_0=0.88\pm0.01$ indicates $J_2/J_1\geq0.9$ and probably close to 1.

Based on "Goodenough rules," Whangbo *et al.*[13] argued that the superexchange parameter J_a in Fig. 1 should be the dominating one, i.e., larger than J_1 and that J_2 is much smaller than J_1 or J_a. This suggests that the tetrahedral unit consisting of the four Cu spins coupled by (J_b,J_a) might be a more advantageous choice than that specified by the (J_1,J_2) interaction lines. The previous analyses do not distinguish between which tetrahedral unit is tetramerized, whereas the present results for the ordered magnetic structures are depending on this choice. The alternative tetrahedral unit predicts ordered structures similar to the one observed except for one essential difference—that the polarization of the spins at sites Cu-3 and Cu-4 are interchanged. This difficulty is so severe that the choice of the (J_b,J_a) tetrahedron as the tetramerized unit must be rejected. The knowledge that J_2 is of the order of J_1 opens up for the alternative possibility for a tetrahedral unit along the c axis in which J_k replaces J_1, but this choice may immediately be dismissed, since this would produce a (nearly) antiferromagnetic ordering of $\langle\mathbf{S}_1\rangle$ and $\langle\mathbf{S}_2\rangle$, if J_k is smaller than J_2, whereas the opposite choice would produce a structure where all phase angles $|\psi_\alpha|<\pi/4$. Hence, it may be concluded that not only is the (J_1,J_2) tetrahedral unit the most natural choice, when considering the distances between the Cu ions, but it is also the only one capable of producing a magnetic structure similar to the one observed.

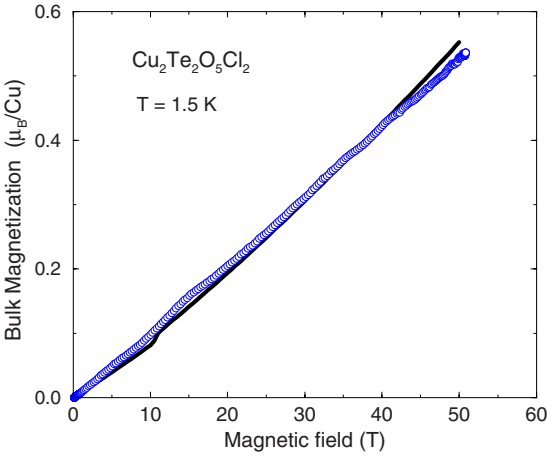

FIG. 2. (Color online) High-field magnetization of $Cu_2Te_2O_5Cl_2$ measured by Gros *et al.* (Ref. 7). The solid line is the calculated result.

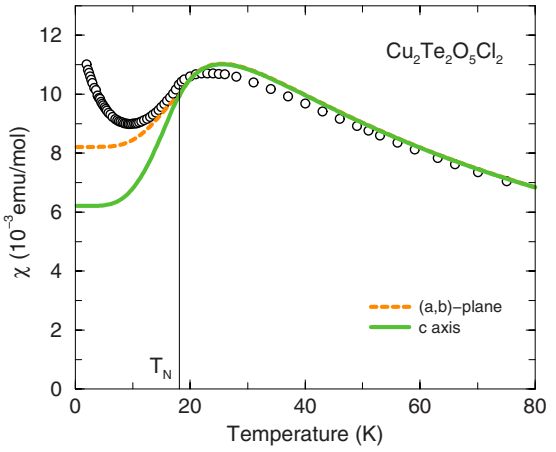

FIG. 3. (Color online) The temperature dependent susceptibility of a polycrystalline sample of $Cu_2Te_2O_5Cl_2$ measured by Lemmens *et al.* (Ref. 3). The experimental results have been scaled so to approach the theoretical ($g=2$) high-temperature value of $0.7503/T$[K] emu/mol. The lines are the calculated components parallel (solid green line) and perpendicular (dashed orange line) to the c axis.

The band-structure calculations of Valentí *et al.*[14] show that most of the electron hopping integrals between the Cu ions connected by the interaction lines in Fig. 1 are significant. This suggests that the corresponding exchange integrals are also important. In accordance with this analysis and with the estimate of Whangbo *et al.*,[13] it is assumed that J_a is the dominating intertetrahedral interaction. For an isolated tetrahedron the ground-state singlet has the energy $-2J_1+\frac{1}{2}J_2$ if $J_1>J_2$ or $-\frac{3}{2}J_2$ in the opposite case, and, in order to secure that (J_1,J_2) is the most favorable tetrahedral unit, J_a has to be smaller than J_1. These considerations indicate that the model value $J_a=0.8J_1$ is reasonable, but I have to stress that the structure calculations themselves are not capable of confirming that this is about the right value. The second largest exchange parameter in the model is the ferromagnetic coupling J_k. The value of this interaction is probably close to being unacceptably large. It is reduced if J_a is increased, but, since J_a may not be that much larger, I have instead introduced the antiferromagnetic J_h interaction along the c axis. The calculated structure does not depend much on J_h-J_k, hence, the assumption of $J_h=0.1J_1$ has effectively reduced the absolute value of J_k by $0.1J_1$. The angle ϕ defining the orientation of the plane of the moments is dictated by the orientation of the DM vectors. The angle between the plane of the moments and the DM vectors is roughly constant, and if assuming the DM vectors to be perpendicular to the vectors connecting the sites involved, i.e., if $\theta_D=33.5°$, the calculated angle ϕ would instead be about $-8°$. The absolute magnitude of the DM coupling is nearly of no importance for the model and is left undetermined. The last one of the 4 extra degrees of freedom has been used for general improvements of the calculated RPA spectrum discussed in Sec. III. The last point I want to discuss is the special role played by the J_f interaction, which accounts effectively for a combination of this interaction with the corresponding interaction between 1,2 (3,4) ions on neighboring tetrahedra along the b (a) axis. Although, the model value of this parameter is small ($-0.03J_1$), it has a strong impact on the calculated structure. The most important reason for introducing J_f has been its great influence on the magnitude of the higher harmonics and the double-**Q** component, which are all nearly eliminated, when introducing $J_f=-0.03J_1$ in combination with a not too small $D_1=0.03J_1$. The uniform magnetization calculated in the presence of an applied field is also significantly improved by the introduction of J_f.

In the case of the final model determined by Eqs. (3) and (9), the calculated magnetization curve at 1.5 K agrees with the experimental one,[7] as shown in Fig. 2. The susceptibility components, assuming an equal population of the two single **Q** domains, are compared to the experimental results obtained from a polycrystalline sample in Fig. 3. The sign and the size of the anisotropy below T_N are in agreement with the experimental results obtained from a single crystal in the antiferromagnetic phase.[15,16] It is somewhat surprising that the bulk exchange parameter $J_B=\Sigma_{\beta j}J_{ij}^{\alpha\beta}=-0.8J_1$ is ferromagnetic, but the least-squares analysis of the bulk properties presented in Ref. 8 led to the same result of $J_B=-0.6J_1$ with an uncertainty of about 20%.

III. MAGNETIC EXCITATIONS IN $Cu_2Te_2O_5Cl_2$

The scattering intensities and energies of the magnetic excitations are calculated for the mean-field model derived in Sec. II. When including the intertetrahedral interactions within RPA, the Cartesian susceptibility tensor of the interacting system is, in real space,[11]

$$\bar{\bar{\chi}}(\alpha i,\beta j)=\bar{\bar{\chi}}^0_{\alpha\beta}(i)\,\delta_{ij}+\sum_{k,\gamma,\eta}\bar{\bar{\chi}}^0_{\alpha\gamma}(i)J_{ik}^{\gamma\eta}\bar{\bar{\chi}}(\eta k,\beta j), \quad (13)$$

where the noninteracting susceptibility tensor is defined by Eq. (6). The frequency argument ω is suppressed but is the same for all the susceptibility tensors. In the present calculations I have neglected the very small contributions of the intertetrahedral classical dipole interaction, which simplification reduces $J_{ik}^{\alpha\beta}$ to a scalar quantity with respect to the Car-

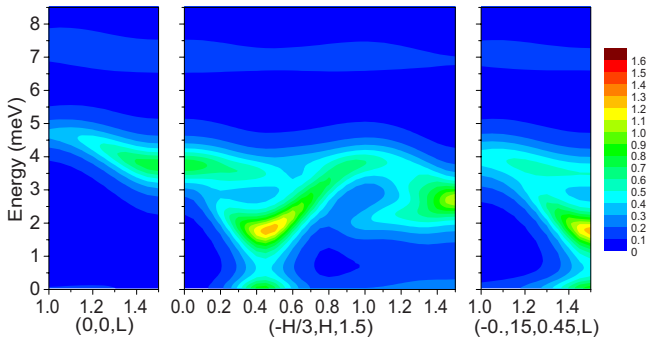

FIG. 4. (Color online) Scattering intensity distributions of the excitations in the paramagnetic phase of $Cu_2Te_2O_5Cl_2$ calculated at 20 K, i.e., contour plots of the correlation function $I(\mathbf{q},\omega)$ in Eq. (16) with $\hbar\epsilon=0.15J_1$.

tesian components. The Fourier transform $J^{\alpha\beta}(\mathbf{q})$ is defined by Eq. (8) and

$$\bar{\bar{\chi}}_{\alpha\beta}(\mathbf{q}) = \sum_k \bar{\bar{\chi}}(\alpha j,\beta k)e^{-i\mathbf{q}\cdot(\mathbf{R}_j-\mathbf{R}_k)}. \tag{14}$$

In the paramagnetic phase $\bar{\bar{\chi}}^0_{\alpha\beta}(j)=\bar{\bar{\chi}}^0_{\alpha\beta}$ is independent of j and the final susceptibility tensor in reciprocal space is determined from

$$\bar{\bar{\chi}}_{\alpha\beta}(\mathbf{q}) = \bar{\bar{\chi}}^0_{\alpha\beta} + \sum_{\gamma\eta} \bar{\bar{\chi}}^0_{\alpha\gamma} J^{\gamma\eta}(\mathbf{q})\bar{\bar{\chi}}_{\eta\beta}(\mathbf{q}). \tag{15}$$

This equation becomes a straightforward matrix equation to be solved with respect to $\bar{\bar{\chi}}_{\alpha\beta}(\mathbf{q})$ when replacing the susceptibility tensors by 12×12 matrices in the vector space spanned by the 3×4 Cartesian components of the four spins in one tetrahedron. The correlation function proportional to the neutron-scattering cross section is then determined by[11]

$$I(\mathbf{q},\omega) = \sum_{\xi\eta} \frac{\delta_{\xi\eta}-q_\xi q_\eta/q^2}{4\pi(1-e^{-\hbar\omega/k_BT})} \sum_{\alpha\beta} \mathrm{Im}[\chi^{\xi\eta}_{\alpha\beta}(\mathbf{q},\omega)e^{-i\mathbf{q}\cdot(\mathbf{r}_\alpha-\mathbf{r}_\beta)}]. \tag{16}$$

The phase factor in the square bracket accounts for the different positions $\mathbf{r}_\alpha=\mathbf{r}_{\alpha j}-\mathbf{R}_j$ of the Cu spins within one tetrahedron. Contour plots of $I(\mathbf{q},\omega)$ calculated for $\mathbf{q}$ along three different directions at 20 K are shown in Fig. 4. The calculations are performed with a finite resolution using $\hbar\epsilon=0.15J_1$ in Eq. (6).

For the noninteracting tetrahedron, when leaving out the small anisotropy terms, the energy differences between the singlet ground state $|s_1\rangle$ and the excited states are $2(1-r)J_1$ to a singlet $|s_2\rangle$, J_1 to a one triplet state $|t_1\rangle$, $(2-r)J_1$ to two degenerate triplets $|t_2\rangle$ and $|t_3\rangle$, and $3J_1$ to a quintuplet $|q\rangle$, where the ratio $r=J_2/J_1$. In the present case of $r=1$, the ground state is doubly degenerated and there are three excited triplets at J_1 and the quintuplet at $3J_1$. At zero temperature, the noninteracting susceptibility of this system only contains one pole at the energy $J_1\simeq3.5$ meV. At 20 K the triplet states are significantly populated implying that the noninteracting susceptibility contains two more poles: one at zero energy and one at $3J_1-J_1$ with intensities of the order 12%–15% of the singlet-triplet-excitation intensity. The anisotropy terms lead to slight modifications of this picture by splitting the degenerate levels into singlets and doublets, but these energy separations are small. The most important feature in the calculated excitation spectra is the singlet-triplet excitation. Due to the intertetrahedral interactions, this becomes a dispersive mode centered around 3.5 meV. The dispersion is strong, when $\mathbf{q}$ is approaching $\mathbf{Q}$ or $\mathbf{Q}_\perp$, where the mode nearly goes soft (20 K is less than 2 K above T_N). The additional poles in the noninteracting susceptibility, due to the thermal population of the triplet states, lead to a weak-intensity excitation branch at about 7 meV and prevent a true soft-mode behavior of the low-energy excitations. The most important correction to this RPA theory is that the excitations acquire a nonzero linewidth due to the single-site fluctuations in the population factors. Based on the diagrammatic high-density $1/z$ expansion,[11,17] a rough estimate of this effect at 20 K shows that it corresponds to that produced by a nonzero value of $\hbar\epsilon\approx0.2J_1$, i.e., close to the value of $\hbar\epsilon=0.15J_1$ used in the calculations. This estimate applies for the singlet-triplet excitations, whereas the excited-states effects are anticipated to be broadened even more. The inelastic neutron-scattering results of Prša *et al.*[18] agree in many details with the calculated dispersive behavior of the triplet excitation. Their results do not include the low-energy part of the spectra, as measurements below 1.4 meV were not possible because of incoherent scattering, and the results do not show any indications of the higher-lying excited-state excitation.

The RPA theory of the ordered phase is more complicated because $\bar{\bar{\chi}}^0_{\alpha\beta}(j)$ changes from one tetrahedron to the next within one commensurable period. In this case we have to apply the following Fourier transforms of the susceptibilities:

$$\bar{\bar{\chi}}^0_{\alpha\beta}(\mathbf{Q}_\mathbf{p}) = \frac{1}{N}\sum_j \bar{\bar{\chi}}^0_{\alpha\beta}(j)e^{-i\mathbf{Q}_\mathbf{p}\cdot\mathbf{R}_j},$$

$$\bar{\bar{\chi}}_{\alpha\beta}(\mathbf{q},\mathbf{Q}_\mathbf{p}) = \frac{1}{N}\sum_{jk} \bar{\bar{\chi}}(\alpha j,\beta k)e^{-i[\mathbf{q}\cdot(\mathbf{R}_j-\mathbf{R}_k)+\mathbf{Q}_\mathbf{p}\cdot\mathbf{R}_j]}, \tag{17}$$

where $\mathbf{Q}_\mathbf{p}$ is one of the $7\times7\times2$ wave vectors of the higher harmonics defined by Eq. (12). In this case the Fourier transform of Eq. (13) is

$$\bar{\bar{\chi}}_{\alpha\beta}(\mathbf{q},\mathbf{Q}_\mathbf{p}) = \bar{\bar{\chi}}^0_{\alpha\beta}(\mathbf{Q}_\mathbf{p}) + \sum_{\mathbf{Q}_\mathbf{s}}\sum_{\gamma\eta} \bar{\bar{\chi}}^0_{\alpha\gamma}(\mathbf{Q}_\mathbf{p}-\mathbf{Q}_\mathbf{s}) \times J^{\gamma\eta}(\mathbf{q}+\mathbf{Q}_\mathbf{s})\bar{\bar{\chi}}_{\eta\beta}(\mathbf{q},\mathbf{Q}_\mathbf{s}). \tag{18}$$

This equation may be solved in a similar way as in the paramagnetic case by transforming to a vector space defined by the 3×4 spin components times the 98 different $\mathbf{Q}_\mathbf{p}$ components. As the ordered structure is nearly determined alone by the principal harmonic, the high dimension of this vector space may to a good approximation be reduced to the one which only involves the 14 $\mathbf{Q}_\mathbf{p}$ components for which the ab components are multiple of the ab component of the ordering wave vector $\mathbf{Q}$ (modulo a reciprocal wave vector). Solving the equation with respect to $\bar{\bar{\chi}}_{\alpha\beta}(\mathbf{q},\mathbf{Q}_\mathbf{p})$ the correlation function $I(\mathbf{q},\omega)$ is determined by the same expression as

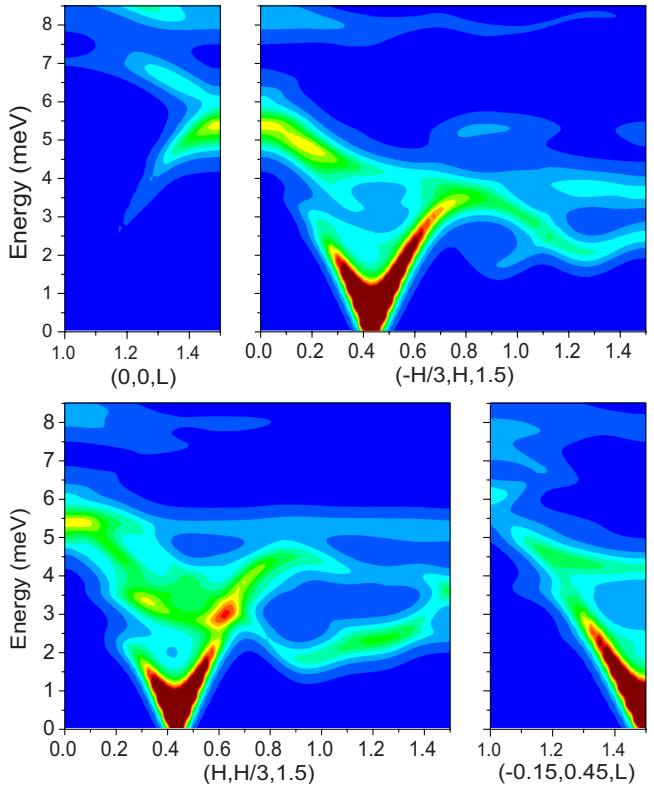

FIG. 5. (Color online) Calculated intensity distributions of the excitations in the ordered phase of $Cu_2Te_2O_5Cl_2$ at 2 K. The resolution, intensity scale, and wave vectors are the same as in Fig. 4. The wave vector $(H,H/3,L)$ is the equivalent of $(-H/3,H,L)$ within the $\mathbf{Q}_\perp$ domain. If both domains are equally populated in the sample, the experimental scattering intensities would be the average of the two cases.

above [Eq. (16)], with $\bar{\bar{\chi}}_{\alpha\beta}(\mathbf{q},\omega)$ being replaced by $\bar{\bar{\chi}}_{\alpha\beta}(\mathbf{q},\mathbf{Q_p}=\mathbf{0},\omega)$.

Selected contour plots of $I(\mathbf{q},\omega)$ in the ordered phase at 2 K are presented in Fig. 5. The noninteracting susceptibility $\bar{\bar{\chi}}^0_{\alpha\beta}(0)$ contains seven different poles but is found to be dominated by two nearly degenerated modes at 5.6 and 6.1 meV. This leads to one major branch as in the paramagnetic case plus some additional modes, which are weak but still visible in the calculated results. The average of the scattering over $\mathbf{q}$ space is expected to be a broad peak centered at about 6 meV, which is in accordance with the experimental results obtained by Crowe *et al.*[19] on a polycrystalline sample. The presence of the DM anisotropy (and the classical dipole interaction) implies that the Hamiltonian does not commute with the generator of an infinitesimal change in the absolute phase ψ_1 of the ordered structure. Hence, the system is not bound to contain a Goldstone mode, a linear dispersive phason mode starting out from a magnetic Bragg point.[20] However, when the system is incommensurably ordered, there should still be a diffusive elastic mode with a diverging intensity at the magnetic Bragg points because of the independence of the free energy to a change in the absolute phase of the ordered structure. This situation has many similarities with the conditions found in the pressure-induced ordered phase of Pr metal.[21] Because the DM anisotropy of the present model is weak and the commensurable period applied in the model is relatively long (close to incommensurability), the calculations show that the system contains a Goldstone-type mode, the intensity of which is strongly increasing when the wave vector is approaching $\mathbf{Q}$. The refined calculation in Fig. 6 shows that the linear dispersive mode is destroyed in the neighborhood of the magnetic Bragg point and is replaced by a diffusive elastic mode in combination with an inelastic "amplitude mode" with an energy gap of about 0.6 meV (the amplitude mode is the out-of-phase excitation deriving from the coupling of the modes at $\mathbf{q}\approx\mathbf{Q}$ and at $\mathbf{q}-2\mathbf{Q}$). The calculations indicate that the scattering intensities resulting from the two domains are quite similar, in particular, the intensities and energies of the excitations propagating along $(H,H/3,3/2)$ are found to be nearly as calculated for the excitations propagating along $(-H/3,H,3/2)$. As discussed above, the excitations exhibit a Goldstone-type behavior, when $\mathbf{q}$ approaches $\mathbf{Q}$, i.e., when $H\rightarrow 0.422$ for the $(-H/3,H,3/2)$ excitations, but it is unexpected that the excitations should show nearly the same behavior when $\mathbf{q}$ approaches the ordering wave vector $\mathbf{Q}_\perp$ of the other domain. As mentioned in connection with the discussion of the strong tendency of the system to create a double-$\mathbf{Q}$ component, the softening of the excitations close to $\mathbf{Q}_\perp$ indicates that the system is close the borderline of the double-$\mathbf{Q}$ phase. The refined results for the scattering intensities in Fig. 6 show that there is one difference between the two cases, as there is only a low-energy inelastic mode—no diffusive elastic scattering near $\mathbf{Q}_\perp$. Notice that the excitation gap at $\mathbf{Q}_\perp$ is actually smaller than the gap displayed by the amplitude mode at $\mathbf{Q}$.

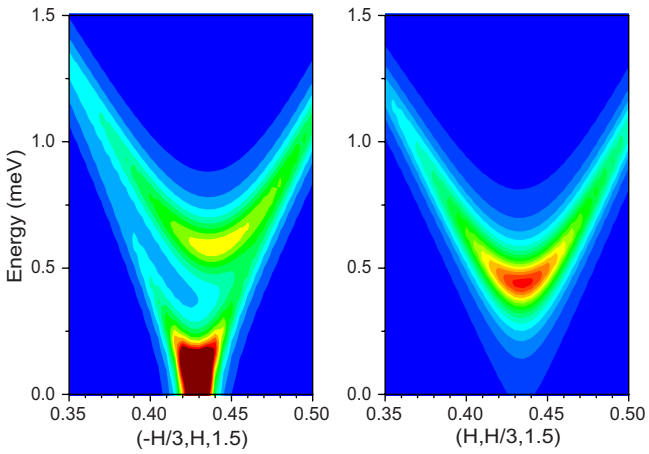

FIG. 6. (Color online) The figure shows parts of the same results as in the previous Fig. 5, except that the scale and resolution ($\hbar\epsilon=0.03J_1$) has been changed in order to show the detail behavior close to the ordering wave vector $\mathbf{Q}=(-\frac{1}{7},\frac{3}{7},\frac{3}{2})$ (left figure) and at the corresponding wave vector $\mathbf{Q}_\perp$ perpendicular to $\mathbf{Q}$ (right figure).

The calculated results show many similarities with the experimental observations.[18] The experiments have resolved the presence of a linear dispersive mode approaching zero energy at the ordering wave vector, but the intensity of this Goldstone mode is weak and is dominated by a mode with a gap of about 2 meV at $\mathbf{q}\approx\mathbf{Q}$, much larger than the energy

gap of about 0.6 meV predicted by the present model. In principle, the RPA theory is capable of reproducing the experimental energy gaps of 2.5 meV at $\mathbf{Q}$ and about 1.9 meV at $\mathbf{Q}_\perp$ by assuming a much stronger DM interaction. In the case of the modified model with $D_1=0.4J_1$, plus minor changes in some of the other parameters $\theta_D=65°$, $J_c=0.2$, $J_d=-0.24$, $J_f=J_h=0$, and $J_k=-0.38$, the only important modification of the calculated ordered structure is that the tilting angle $|\theta_1|$ (but not $|\theta_3|$) now becomes of an appreciable magnitude of about 15°. The intensity of the third harmonic is increased but is still 300 times smaller than the main peak. In most cases, the modified model predicts nearly the same inelastic-scattering intensities as shown above. The only distinct change is that the low-energy modes in the ordered phase near $\mathbf{Q}$ and $\mathbf{Q}_\perp$ are now predicted to occur at about 2.1 and 1.4 meV, respectively, i.e., approaching the experimental values. Within RPA, the large gap at $\mathbf{Q}$ may only occur if the system is strongly anisotropic, however, the large magnitude of the DM interaction in the modified model, being of the same order of magnitude as the exchange integral, seems unrealistic. Except for this low-energy phenomenon, the RPA theory in combination with the MF model derived in Sec. II produces results which agree reasonably with the observations. There are a number of clear quantitative deviations with respect to the energies of the excitations which are also outside the near neighborhoods of the magnetic Bragg points. I have tried to reduce these discrepancies, but the conditions set by the fitting of the ground-state properties do not leave much room for improvements of the RPA spectra.

The Raman spectra of $Cu_2Te_2O_5Cl_2$ were recently measured by Choi *et al.*[16] The magnetic part of the Raman-scattering cross section is dominated by non-spin-flip scattering from longitudinal excitations at zero wave vector. The magnetic Raman scattering of the present model has been calculated using the procedure developed in Ref. 8, and in the ordered phase it is found to be dominated by peaks at 3.8 and 7.9 meV (31 and 64 cm^{-1}) of about equal intensities. The lower peak is lying too low in energy whereas the position of the upper one agrees with the experimental low-temperature observations,[16] which show two equal-sized peaks at 49 and 67 cm^{-1} plus an extra one only appearing in the (cc) scan at 39 cm^{-1}.

IV. MF/RPA THEORY FOR $Cu_2Te_2O_5Br_2$

The MF/RPA model for the Br compound has been constructed by following the same steps as used above. The intratetrahedral interactions are

$$J_1 = 47.5 \text{ K}, \quad J_2 = 0.7J_1, \quad D_1 = 0.03J_1, \quad \theta_D = 33.2°, \tag{19}$$

whereas the intertetrahedral exchange-interaction parameters are somewhat smaller than in the Cl case,

$$J_a = 0.17, \quad J_b = 0.33, \quad J_c = 0.1, \quad J_d = -0.35,$$

$$J_f = -0.1, \quad J_h = 0.1, \quad J_k = -0.22, \tag{20}$$

in units of J_1 for the Br compound. This model produces susceptibility and high-field magnetization curves in reasonable agreement with experiments (see Ref. 8). The ordering wave vector is $\mathbf{Q}=(-0.172, 0.356, 0.5)$ and in the calculations this wave vector is approximated by the commensurable value $(-\frac{1}{6}, \frac{1}{3}, \frac{1}{2})=(-0.167, 0.333, 0.5)$. The calculated ordered structure is described by Eq. (10), and the characteristic parameters calculated at 2 K are compared with the experimental ones of Zaharko *et al.*[6] in the lower part of Table I. The calculated spin structure in the Br compound is slightly closer to the "nonfrustrated" helix ($\theta_1=\theta_2=0$, $\psi_2=0$, and $\psi_3=\psi_4=\pm 180°$) than it is in the Cl system, whereas the experimental results show the opposite trend. The neutron-diffraction measurements indicate that the angle α_{34} between the spins of the Cu-3 and Cu-4 ions in the Br system at 2 K is as large as 120°, whereas the calculated value is $\alpha_{34} \simeq 30°$. This major discrepancy indicates that the present Br model should be considered as a preliminary one, the predictions of which may not be entirely reliable.

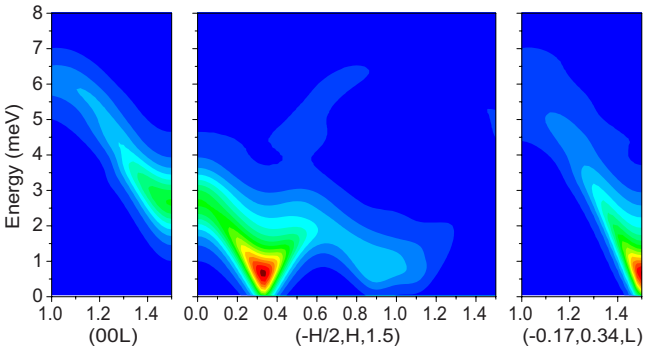

FIG. 7. (Color online) Calculated intensity distributions of the excitations in the ordered phase of $Cu_2Te_2O_5Br_2$ at 2 K. The resolution is $\hbar\epsilon=0.15J_1$.

The intertetrahedral spin interactions produce an exchange field which is only about 15% larger than that required for inducing the ordered state and the amplitude of the ordered spin is only 0.2 at 2 K. As in the Cl case, this amplitude depends on the ratio $r=J_2/J_1$ and once more the spin amplitude is indicating a value of r (=0.7 in this case), which is in agreement with that estimated by the previous analysis.[8]

The paramagnetic excitation spectra of the Br compound are calculated to be qualitatively similar to the results shown in Fig. 4 for the Cl model. The differences are that the singlet-triplet splitting determined by J_1 is increased by 15%, but the bandwidth determined by the intertetrahedral interactions is nearly a factor of 2 more narrow. The noninteracting susceptibility of the Br system in the ordered phase at 2 K (and 7 K) is completely dominated by a single pole at 4.3 meV. The position of this pole is in agreement with that the scattering intensities integrated over q space is showing a peak centered at 4.2 meV at 7 K or at about 5 meV at 8 K.[19,22] The single-pole dominance implies that the calculated excitation spectra show fewer extra branches than found in the Cl system. In most other respects, the calculated scattering intensities in the ordered phase of the Br system behave nearly as in the Cl case [see Fig. 7]. The fine resolution results for the Goldstone-type modes in the neighborhood of $\mathbf{Q}$ and $\mathbf{Q}_\perp$ compare closely to the results shown in Fig. 6 for the Cl model. The calculated energy gap of the amplitude

mode is about 0.75 meV slightly larger than the 0.6 meV of the Cl system. The energy gap at $\mathbf{Q}_\perp$ is nearly the same; not smaller like in the Cl compound. In the present system the similarities of the two spectra along $(-H/2,H,1.5)$ and $(H,H/2,1.5)$ are mostly due to the small amplitude of the ordered moments (the two wave vector directions become identical in the limit of zero amplitude). In contrast to the model for the Cl system, the present one does not show any tendency toward a double-**Q** ordering.

The calculated Raman-scattering cross section of the Br system at 2 K agrees qualitatively with the one derived from the simple model in Ref. 8 by showing a strong peak at 1.7 meV and a weak but strongly field dependent one at 2.7 meV (14 and 21 cm^{-1}). This result is in good agreement with experiments[3,7,8] except that the two peaks are observed at slightly higher energies (16 and 24 cm^{-1}).

V. DISCUSSION

The present analysis is based on the simplest approximations, MF and RPA, but starts out from a cluster unit comprising four 1/2 spins. This means that the local effective spin has as many degrees of freedom as in the case of, for example, Dy^{3+}. The present RPA is the equivalent of linear spin-wave theory. The nonlinear quantum corrections to the theory are important for $S=1/2$, but, because they scale with the factor $(2S)^{-1}$, they should not disqualify the present approach where $2S_{\mathrm{eff}}+1=16$. It was originally anticipated that the interactions between the tetrahedral spins in this compound should have a low-dimensional character. This is not the case as the tetrahedral units are strongly coupled with each other not only in the *ab* plane but also along the *c* axis. One may argue that this conclusion is an artifact of the simplified analysis. However, the experimental behavior of the susceptibility and the heat capacity indicates that the effective $J(\mathbf{Q})$ of $Cu_2Te_2O_5Cl_2$ has to be of the order of $2J_1$ and the ordering wave vector is incommensurable, all of which may only be achieved by an interaction scheme similar to the one derived in the present analysis. The interacting system must be characterized as a three-dimensional one with a coordination number which is comparable to that of an hcp/fcc lattice. An equivalent conclusion is reached by Jagličić *et al.*,[23] who did not find any sign of broken-ergodicity properties of $Cu_2Te_2O_5Cl_2$.

The large effective *S* of the tetramerized cluster spins and the three-dimensional interaction scheme make the present magnetic systems similar to that of a rare-earth metal for which the magnetic properties are well described in terms of the diagrammatic $1/z$ expansion.[11,17] The leading order approximation in this expansion is the MF/RPA theory, and the most important higher-order corrections are the line broadening of the excitations due to single-site fluctuations plus a 10%–15% renormalization of the bare interaction parameters. This theory gives an adequate description of the excitations in the slightly undercritical Pr metal.[11,21,24] In this singlet-doublet system, the excitations remain reasonably well defined up to a relative temperature $t=T/T_\Delta \approx 1$, where T_Δ is the temperature corresponding to the noninteracting energy gap of the excited state. The inelastic-scattering experiments of Prša *et al.*[18] show that the singlet-triplet excitations are still visible in the two Cu systems at $t \simeq 0.5$ ($T=20$ K), but that they more or less disappear above this temperature (at least close to the ordering wave vector). In these systems the higher multiplicity of close lying excited states (a singlet and three triplets) is going to increase the linewidths and to reduce the intensities and the dispersion of the paramagnetic singlet-triplet excitations in comparison with Pr metal at the same relative temperature *t*. Hence, although the renormalization effects are stronger in these tetramerized singlet-triplet systems than in Pr metal, it is likely that most of their paramagnetic properties may be explained by the $1/z$ expansion to first order in *z*.

The spin cluster units are distorted tetrahedra, nevertheless, the analysis indicates that $J_2/J_1 \approx 1$ in the case of $Cu_2Te_2O_5Cl_2$ suggesting that the ground state of the isolated clusters is, accidentally, nearly doubly degenerated. This degeneracy does not compare with the one occurring in the geometrically frustrated pyrochlore antiferromagnets,[2] where the tetrahedra are sharing corners. In the present system the interactions between the different tetrahedral clusters should imply that there is a unique magnetic ground state with the reservation that the model calculations suggest—that the free energies of the single- and double-**Q** structures are nearly equal in the Cl system. The Br system does not share the two degeneracies. $J_2/J_1=0.7$ and the model calculations do not show any tendency toward a double-**Q** ordering of the Br compound. The magnetic properties of the two systems only differ to the extent expected from the different strengths of the interactions, which circumstance indicates that the two accidental degeneracies of the Cl system do not cause any additional frustrationlike effects of importance.

The intratetrahedral exchange parameters, J_1 and J_2, derived from the analysis of the two tetramerized Cu systems are trustworthy. Experimental uncertainties combined with the difficulties in reproducing all details of the ordered structures and of the excitation spectra, particularly in the case of the Br compound, imply that the intertetrahedral exchange parameters are much more uncertain. The magnetic structures in the two Cu systems are close being simple tilted helical structures and if the DM anisotropy is neglected the systems should show a Goldstone mode. In principle, the DM anisotropy is expected to be weak of the order of a few percent of the isotropic interaction. The diffraction experiments do not reveal any strong scattering from higher harmonics,[6,12] which is indirectly verifying that the anisotropy is small. This is also indicated by the incommensurable values of the ordering wave vectors. The MF models developed here are in accordance with these conditions and they predict a strong Goldstone-type mode and a weak-intensity amplitude mode at rather low energy. The inelastic-scattering results[18] contradict this picture by showing a strongly gapped amplitude mode of large intensity and only a weak indication of the phason mode close to the magnetic Bragg point.

It is difficult to explain this discrepancy. Experimentally, a high level of defects may be of importance since anything that tends to clamp the ordered structure is going to increase the gap at **Q**. That the quality of the crystals is no trivial matter is indicated by, for instance, the observation[5] of two different ordering wave vectors in one of the $Cu_2Te_2O_5Cl_2$

crystals, at $\mathbf{Q}=\mathbf{k}'=(-0.15,0.42.0.5)$ and at $\mathbf{k}=(0.15,0.42.0.5)$. It is unlikely that the DM anisotropy is much stronger than the value of $0.03J_1$ assumed in the present models. As discussed by Zorko *et al.*[25] the DM anisotropy of [two-dimensionally (2D) frustrated] Cu systems is found to lie in the range of 4%–16% of the exchange. An increase in the DM anisotropy of the present systems by about a factor of 5, $D_1 \simeq 0.16J_1$ instead of $0.03J_1$, does not remove the discrepancy. The energy gap of the amplitude mode at the ordering wave vector is still a factor of 2 smaller than observed, and the intensity of this mode remains weak compared to that of the phason mode. The anisotropy due to orbital modifications of the $S=\frac{1}{2}$ state of the $3d^9$ configuration of the Cu^{++} ions is also expected to be moderate. Torque magnetometric measurements of the anisotropy of the susceptibility by Miljak and Herak[26] show that the anisotropy is zero within the *ab* plane in the paramagnetic phase. The difference between the *c* axis and *a* or *b* axes susceptibility components of $Cu_2Te_2O_5Cl_2$ is about -1.3×10^{-3} emu/mol at T_N, and, when the system is heated, the difference decreases in proportion to the reduction in the averaged susceptibility and is about -0.42×10^{-3} emu/mol at 200 K. This behavior is accounted for by a constant *g* factor anisotropy, $g_c^2-g_a^2\approx-0.12g_{\mathrm{eff}}^2$, with no need for introducing any further axial spin anisotropy.

The two systems are frustrated due to the competition between the intra- and intertetrahedral spin interactions. This frustration is reflected in that the spin configuration of the single tetrahedra deviate from the optimal one of $\langle\mathbf{S}_1\rangle$ and $\langle\mathbf{S}_2\rangle$ being parallel and antiparallel to $\langle\mathbf{S}_3\rangle$ and $\langle\mathbf{S}_4\rangle$. The MF/RPA approximations may not be trusted in the case of strong frustration, however, the most important parts of the frustration effects are those originating from the strong intratetrahedral interactions, which are included in an exact way in the theory.

ACKNOWLEDGMENTS

Henrik Rønnow, Krunoslav Prša, Niels Bech Christensen, and Oksana Zaharko are gratefully acknowledged for many stimulating discussions and for providing me with their neutron-scattering data prior to publication. The correspondence with Mladen Prester and the report on the unpublished susceptibility measurements by Marko Miljak and Mirta Herak have been of great value. It is a pleasure to thank Maged Elhajal, Frédéric Mila, and Sonya Crowe for helpful comments and discussions.

[1] M. Johnsson, K. W. Törnroos, F. Mila, and P. Millet, Chem. Mater. **12**, 2853 (2000).
[2] S. T. Bramwell and M. J. P. Gingras, Science **294**, 1495 (2001).
[3] P. Lemmens, K. Y. Choi, E. E. Kaul, C. Geibel, K. Becker, W. Brenig, R. Valentí, C. Gros, M. Johnsson, P. Millet, and F. Mila, Phys. Rev. Lett. **87**, 227201 (2001).
[4] P. Lemmens, K. Y. Choi, A. Ionescu, J. Pommer, G. Güntherodt, R. Valentí, C. Gros, W. Brenig, M. Johnsson, P. Millet, and F. Mila, J. Phys. Chem. Solids **63**, 1115 (2002).
[5] O. Zaharko, A. Daoud-Aladine, S. Streule, J. Mesot, P. J. Brown, and H. Berger, Phys. Rev. Lett. **93**, 217206 (2004).
[6] O. Zaharko, H. Rønnow, J. Mesot, S. J. Crowe, P. J. Brown, A. Daoud-Aladine, A. Meents, A. Wagner, M. Prester, H. Berger, and D. M. Paul, Phys. Rev. B **73**, 064422 (2006).
[7] C. Gros, P. Lemmens, M. Vojta, R. Valentí, K. Y. Choi, H. Kageyama, Z. Hiroi, N. V. Mushnikov, T. Goto, M. Johnsson, and P. Millet, Phys. Rev. B **67**, 174405 (2003).
[8] J. Jensen, P. Lemmens, and C. Gros, Europhys. Lett. **64**, 689 (2003).
[9] M. Elhajal and F. Mila (private communication).
[10] T. Moriya, Phys. Rev. **120**, 91 (1960).
[11] J. Jensen and A. R. Mackintosh, *Rare Earth Magnetism: Structures and Excitations* (Clarendon, Oxford, 1991); http://www.nbi.ku.dk/page40667.htm
[12] O. Zaharko (private communication).
[13] M.-H. Whangbo, H.-J. Koo, and D. Dai, Inorg. Chem. **42**, 3898 (2003).
[14] R. Valentí, T. Saha-Dasgupta, C. Gros, and H. Rosner, Phys. Rev. B **67**, 245110 (2003).
[15] M. Prester, A. Smontara, I. Zivkovic, A. Bilusic, D. Drobac, H. Berger, and F. Bussy, Phys. Rev. B **69**, 180401(R) (2004).
[16] K. Y. Choi, H. Nojiri, N. S. Dalal, H. Berger, W. Brenig, and P. Lemmens, arXiv:0806.0147, Phys. Rev. B (to be published).
[17] R. B. Stinchcombe, J. Phys. C **6**, 2459 (1973).
[18] K. Prša, H. M. Rønnow, O. Zaharko, N. B. Christensen, J. Jensen, J. Chang, S. Streule, M. Jiménez-Ruiz, H. Berger, M. Prester, and J. Mesot (unpublished).
[19] S. J. Crowe, S. Majumdar, M. R. Lees, D. McK. Paul, R. I. Bewley, S. J. Levett, and C. Ritter, Phys. Rev. B **71**, 224430 (2005).
[20] D. Forster, *Hydrodynamic Fluctuations, Broken Symmetry, and Correlation Functions* (Benjamin, London, 1975).
[21] J. Jensen, K. A. McEwen, and W. G. Stirling, Phys. Rev. B **35**, 3327 (1987).
[22] S. J. Crowe, S. Majumdar, M. R. Lees, D. McK. Paul, D. T. Adroja, and S. J. Levett, Physica B **359-361**, 1219 (2005).
[23] Z. Jagličić, S. El Shawish, A. Jeromen, A. Bilušić, A. Smontara, Z. Trontelj, J. Bonča, J. Dolinšek, and H. Berger, Phys. Rev. B **73**, 214408 (2006).
[24] P. Bak, Phys. Rev. B **12**, 5203 (1975).
[25] A. Zorko, S. Nellutla, J. van Tol, L. C. Brunel, F. Bert, F. Duc, J.-C. Trombe, M. A. de Vries, A. Harrison, and P. Mendels, Phys. Rev. Lett. **101**, 026405 (2008).
[26] M. Miljak and M. Herak (unpublished).